Proceedings of the 12th Workshop on Quantum Chaos and Localisation Phenomena (CHAOS 25)

Stability of Higher-Order Spacing Ratios for Poisson and Semi-Poisson Ensembles with Missing Levels

A. Akhshani* and L. Sirko

Institute of Physics, Polish Academy of Sciences, al. Lotników 32/46, PL-02668 Warszawa, Poland

Doi: 10.12693/APhysPolA.148.S31 *e-mail: akhshani@ifpan.edu.pl

We investigate the impact of random level loss on the higher-order level spacing ratio statistics, $P^{(k)}(r)$, of Poisson and semi-Poisson ensembles. By employing the Wasserstein distance to quantify distributional changes, we show that the two ensembles exhibit different responses to missing levels. The statistics of the Poisson ensemble are stable, with the distributions remaining invariant in the presence of missing levels. The Wasserstein distance between complete and incomplete spectra remains at the level of the numerical noise floor. However, the semi-Poisson ensemble demonstrates substantial statistical instability. Eliminating levels alters the distributions, yielding a measurable discrepancy, assessed by Wasserstein distance, which is 100 times greater than the associated numerical noise. The folded ratio distribution, $P^{(k)}(\tilde{r})$, is the most effective method for probing the instability signal, which, as we show, is significantly amplified at higher orders ($k > 1$). These findings clarify a key uncertainty in spectral analysis, wherein a degraded semi-Poisson spectrum may be erroneously identified as a Poisson one. The stability of a spectrum's statistics in response to the artificial removal of levels serves as a robust, model-independent test for differentiating between uncorrelated and correlated quantum systems, turning the problem of missing levels into a powerful diagnostic feature.

topics: higher-order spacing ratios, missing levels, Poisson and semi-Poisson ensembles, Wasserstein distance

1. Introduction

Quantum chaos, the study of quantum systems that have chaotic classical counterparts, has shown deep links between the statistical properties of quantum energy spectra and the nature of the underlying classical motion [1–4]. This connection is built upon two foundational conjectures. The Bohigas–Giannoni–Schmit (BGS) conjecture suggests that the spectral fluctuations of chaotic quantum systems are thoroughly characterized by random matrix theory (RMT) [5, 6]. The global symmetries of the Hamiltonian fully determine the specific RMT ensemble, which may be a Gaussian orthogonal (GOE) [7–9], unitary (GUE) [10, 11], or symplectic (GSE) [12–15] ensemble. On the other hand, the Berry–Tabor conjecture proposes that the spectra of classically integrable systems are uncorrelated and follow Poisson statistics [16]. The duality of RMT for chaos and Poisson for integrability serves as a fundamental basis in spectral analysis in quantum chaos and related fields, providing a robust framework for identifying the underlying dynamics of complex quantum systems by means of their eigenvalue sequences. Additionally, physical systems can show dynamics that are neither fully chaotic nor integrable [17–19]. These systems, known as pseudo-integrable, exhibit statistical properties that deviate from both RMT and Poisson predictions, leading to the investigation of intermediate statistical models such as the semi-Poisson ensemble [20–22].

Conventionally, the primary tool for investigating these spectral statistics has been the nearest-neighbor spacing distribution, $P(s)$, where s denotes the separation between consecutive energy levels. For chaotic systems, $P(s)$ demonstrates level repulsion, meaning the probability of finding small spacings vanishes as $P(s) \approx s^{\beta}$, where β represents the Dyson index ($\beta = 1, 2, 4$ for GOE, GUE, and GSE, respectively) [6]. In integrable systems, the lack of correlation results in level clustering, characterized by the exponential Poisson distribution, $P(s) = \mathrm{e}^{-s}$. The energy spectrum's "unfolding" is a major issue in the practical use of $P(s)$. This procedure normalizes the local energy levels to achieve a mean spacing of one, removing system-specific fluctuations in the average density of states. This demands a precise understanding of the smooth part of the system's density of states, which is often unknown analytically, particularly for interacting many-body systems or in the analysis of experimental data. Different unfolding methodologies

applied to identical raw data can produce disparate statistical outcomes, potentially causing inaccurate physical interpretations [23]. This practical challenge leads to exploring statistical measures that are independent of the local density of states.

To address the methodological challenges and uncertainties associated with spectral unfolding, Oganesyan and Huse proposed the analysis of the ratio of consecutive level spacings [24]. This statistic is defined using the ratio of consecutive level spacings, $r_n = s_n/s_{n-1}$, where $s_n = E_{n+1} - E_n$ denotes the spacing between consecutive energy levels. It is inherently independent of the local density of states because of its construction as a ratio of adjacent spacings, which eliminates the influence of the local mean spacing. This independence ensures that the distribution $P(r)$ does not require the unfolding procedure [25, 26]. Thus, $P(r)$ and its confined variant $P(\tilde{r})$ evaluate short-range correlations, whereas $P^{(k)}(r)$ provides a more robust method for examining the long-range, multi-scale spectral rigidity of the system. Analytical expressions for $P^{(k)}(r)$ have recently been provided for both Poisson and semi-Poisson ensembles [27, 28]. These statistics are sensitive to longer-range spectral correlations and exhibit their own rich structure. For example, our recent study revealed that even uncorrelated Poisson spectra can mirror the characteristics of the RMT ensemble at certain k values (e.g., GUE at $k = 4$), while semi-Poisson statistics display this more quickly (e.g., GUE at $k = 2$) [27].

The completeness of the eigenvalue sequence is a key assumption in many statistical analyses. In practice, in complex experiments or simulations of many-body systems, a fraction of levels may be missed due to inadequate resolution or low coupling strength, resulting in a fraction of energy levels being missed. The occurrence of missing levels is not a trivial effect; it can significantly alter the statistical properties of the correlated spectrum [29–31]. In semi-Poisson statistics, missing levels can reduce the signatures of short-range repulsion. The decay is quantifiable, i.e., the mean of the bounded ratio $\tilde{r} = \min(r, 1/r)$ declines from 0.5 (semi-Poisson) to nearly 0.386 (Poisson) with increasing level loss [17, 25, 26]. In fact, the $P(r)$ statistics itself is ambiguous when missing levels are present. Thus, an observer analyzing a partial semi-Poisson spectrum may inaccurately classify the system as Poissonian, leading to a misrepresentation of the actual dynamics. In this work, we address this fundamental challenge by analyzing the dynamical response of higher-order $P^{(k)}(r)$ statistics for Poisson and semi-Poisson ensembles with respect to the missing levels. To provide a robust, quantitative measure of this response, we use the one-dimensional Wasserstein distance to track deviations of the distributions from their complete forms [32, 33].

2. Higher-order level spacing ratios

This section reviews the established theoretical framework for the higher-order level spacing ratio distributions, $P^{(k)}(r)$. The distributions for the Poisson and semi-Poisson ensembles, which underpin our study, are derived from the fundamental statistical properties of their corresponding level spacings, s [25, 34, 35].

2.1. Definition of the non-overlapping ratio

Let an ordered sequence of energy eigenvalues be denoted by $\{E_n\}$, such that $E_1 \le E_2 \le \cdots \le E_N$. The nearest-neighbor spacing is defined as $s_n = E_{n+1} - E_n$. To probe correlations over longer energy scales, the k-th order spacing, $s_n^{(k)}$, is defined as the span of $k+1$ consecutive levels, i.e.,

$$s_n^{(k)} = E_{n+k} - E_n = \sum_{i=n}^{n+k-1} s_i. \tag{1}$$

To construct a dimensionless, unfolding-free quantity, the ratio of consecutive, non-overlapping k-th order spacings is used, yielding

$$r_n^{(k)} = \frac{s_{n+k}^{(k)}}{s_n^{(k)}} = \frac{E_{n+2k} - E_{n+k}}{E_{n+k} - E_n}. \tag{2}$$

The non-overlapping nature of this definition is crucial — the numerator and denominator are sums over completely distinct sets of elementary spacings. For uncorrelated or weakly correlated spectra, this ensures that they are statistically independent random variables — a property that facilitates the derivation of the probability distribution $P^{(k)}(r)$ [25, 28, 34, 35].

2.2. Poisson ensemble

The Poisson ensemble characterizes the spectral properties of classically integrable systems, identified by uncorrelated energy levels. The corresponding nearest-neighbor spacings follow the exponential distribution, $P(s) = \mathrm{e}^{-s}$. The sum of k spacings, $s^{(k)}$, in a complete Poisson spectrum adheres to a gamma distribution $\Gamma(k, 1)$. The ratio of two independent variables yields the probability distribution for the k-th order ratio [28]

$$P_{\mathrm{P}}^{(k)}(r) = \frac{\Gamma(2k)}{\Gamma(k)^2} \frac{r^{k-1}}{(1+r)^{2k}} = \frac{(2k-1)!}{((k-1)!)^2} \frac{r^{k-1}}{(1+r)^{2k}}. \tag{3}$$

For $k = 1$, (3) simplifies to the well-known distribution $P(r) = 1/(1+r)^2$, which is monotonic and maximal at $r = 0$, reflecting the tendency for level clustering. As k increases, the distribution exhibits

Baseline Wasserstein distances $W(p=0)$ for complete spectra. TABLE I

Distribution	Ensemble	$k=1$	$k=2$	$k=3$	$k=4$
$P^{(k)}(r)$	Poisson	0.00038	0.00039	0.00033	0.00032
	semi-Poisson	0.00039	0.00029	0.00026	0.00025
$P^{(k)}(\tilde{r})$	Poisson	0.00514	0.00018	0.00013	0.00013
	semi-Poisson	0.00017	0.00010	0.00010	0.00011

a peak farther from the origin, indicating an emergent statistical repulsion. Notably, for particular integer values of k, this distribution visually mimics those of RMT ensembles; for $k=4$, it roughly aligns with the GUE statistics, and for $k=7$, it approximates the GSE statistics [27].

2.3. The semi-Poisson ensemble

The semi-Poisson (sP) ensemble characterizes systems exhibiting intermediate dynamics that are neither fully integrable nor chaotic, such as pseudo-integrable billiards. It is derived from the short-range plasma model, where levels interact only with their nearest neighbors. This results in a linear level repulsion, characterized by the nearest-neighbor spacing distribution $P(s) = 4s\,\mathrm{e}^{-2s}$, which follows a gamma distribution $\Gamma(2,2)$. The sum of k spacings, $s^{(k)}$, thus follows a $\Gamma(2k,2)$ distribution. The higher-order distribution for the semi-Poisson ensemble can be defined [27]

$$P_{\mathrm{sP}}^{(k)}(r) = \frac{\Gamma(4k)}{\Gamma(2k)^2}\frac{r^{2k-1}}{(1+r)^{4k}} = \frac{(4k-1)!}{((2k-1)!)^2}\frac{r^{2k-1}}{(1+r)^{4k}}. \quad (4)$$

For $k=1$, (4) results in $P(r) = 6r/(1+r)^4$, demonstrating the characteristic linear repulsion ($P(r) \sim r$) of the sP ensemble. The convergence to behavior that resembles random matrix theory is notably swift. For $k=2$, the distribution closely aligns with the GUE prediction, exhibiting a repulsion of $\sim r^3$. For $k>2$, the distributions become even more sharply peaked around $r=1$ compared to their RMT counterparts [27].

3. The impact of missing levels

In this section, we develop a framework to understand how random level loss impacts the higher-order ratio statistics of the Poisson and semi-Poisson ensembles. We demonstrate how the differential response of Poisson and semi-Poisson ensembles in the presence of missing levels can be leveraged as a powerful diagnostic tool. We present a quantitative analysis of this phenomenon, including a precise characterization of the simulation's baseline noise, and interpret the results to form a clear picture of their diagnostic potential.

We model spectral incompleteness via random level loss. Consider a complete energy level sequence $\mathcal{E} = \{E_n\}$. By independently removing each level with a fixed probability p, we obtain a new sequence, $\mathcal{E}' = \{E'_m\}$, which is less dense than the original. This process fundamentally alters the sequence of nearest-neighbor spacings [36]. A new spacing, $s'_m = E'_{m+1} - E'_m$, is generated in the incomplete sequence across a gap that could have missing levels. As a result, each new spacing s'_m corresponds to the sum of one or more consecutive spacings from the original sequence [37]. We will examine the impact of this random re-summation of spacings on the higher-order ratio distributions.

4. Results of the quantitative analysis: stability vs degradation

We conduct a quantitative assessment by measuring the deviation of a distribution from its ideal form through the application of the one-dimensional Wasserstein distance, $W(p)$ [33]. This metric is calculated for each probability of level loss (p) through a comparison of the probability distribution of the numerically generated spectrum with the ideal analytical distribution for a complete spectrum. The calculation of the baseline "noise floor," $W(p=0)$, for each ensemble is a critical component of our analysis. This value, presented in Table I, indicates the calculated distance between a complete numerical spectrum and its corresponding ideal analytical form. The observed discrepancy between our numerical simulation and the theoretical model can be attributed to finite statistics and binning effects. This value is interpreted as the basic "noise floor" of our simulation. The primary diagnostic involves comparing the distance measured for spectra that have missing levels, $W(p \geq 0)$, against precisely determined baseline $W(p=0)$. A spectrum is considered statistically stable if $W(p>0)$ remains on the order of the noise floor $W(p=0)$, whereas it is classified as unstable if $W(p>0)$ increases significantly and systematically beyond the noise floor.

As noted in Table I, the noise floor for the $k=1$ folded Poisson distribution, $P_P^{(k)}(\tilde{r})$, is significantly high (0.00514). In fact, the transformation from r to $\tilde{r}$ introduces a numerical instability due to the slow $1/r^2$ decay of the $P(r)$ tail, which is challenging to address using standard binning methods.

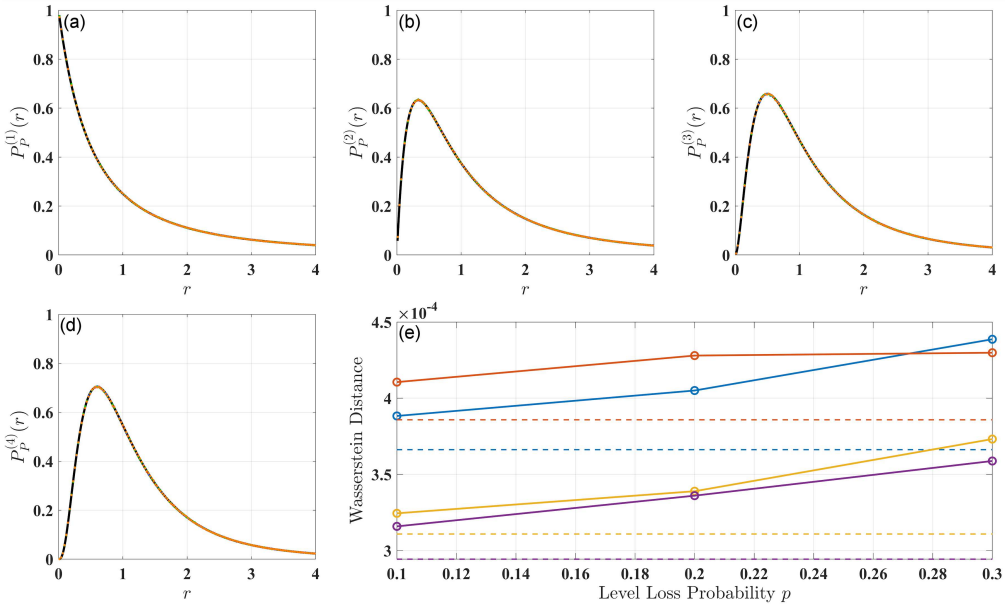

Fig. 1. Stability analysis of the distribution $P_{\mathrm{P}}^{(k)}(r)$ for Poisson ensembles. Panels (a)–(d) illustrate numerical distributions $P_{\mathrm{P}}^{(k)}(r)$ for orders $k = 1$–4 with level loss $p = 0$ (red dots), 0.1 (blue dots), 0.2 (green dots), and 0.3 (orange dots), all in excellent agreement with the analytical curve (solid black line). The obtained distributions overlap with very high accuracy. Panel (e) presents the Wasserstein distance $W_{\mathrm{P}}(p)$. Dashed lines indicate the $W(p = 0)$ noise floor for each k, and the colored trend lines (blue, orange, yellow, purple for $k = 1$–4, respectively) remain at the floor, demonstrating the stability of Poisson statistics in the presence of missing levels.

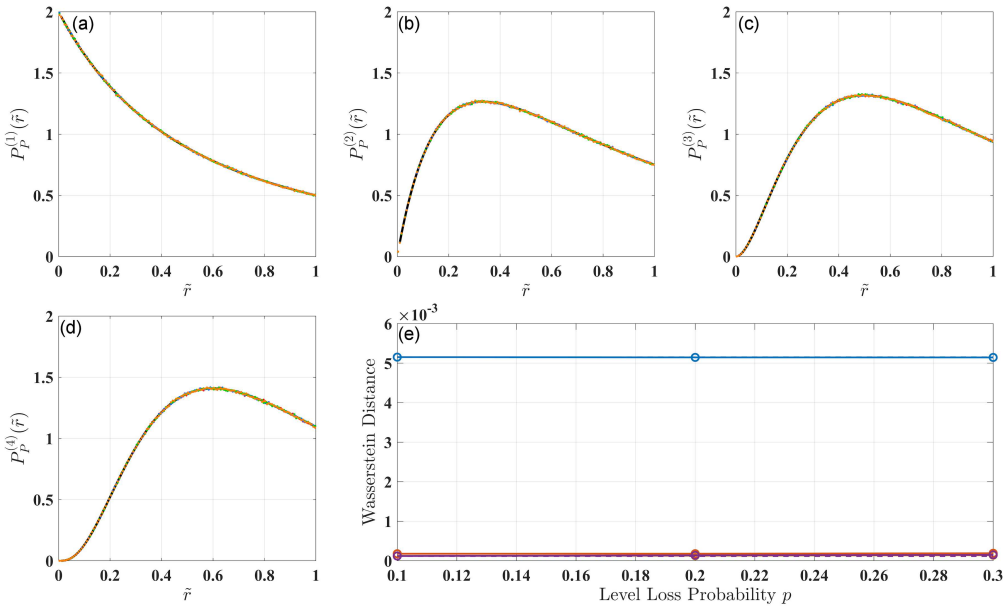

Fig. 2. Stability analysis for the folded distribution $P_{\mathrm{P}}^{(k)}(\tilde{r})$ of the Poisson ensemble. Panels (a)–(d) display the distributions for orders $k = 1, 2, 3, 4$. In each, the numerical distributions for level loss probabilities $p = 0$ (red dots), $p = 0.1$ (blue dots), $p = 0.2$ (green dots), and $p = 0.3$ (orange dots) are statistically indistinguishable and align perfectly with the analytical prediction (solid black line). The summary plot (panel (e)) shows the Wasserstein distance as a function of the level loss probability p. The dashed lines indicate the corresponding $W(p = 0)$ noise floor for each k. For all orders of k, the solid trend lines (blue for $k = 1$, orange for $k = 2$, yellow for $k = 3$, and purple for $k = 4$) are perfectly flat, demonstrating that the folded distributions maintain robust stability in the presence of missing levels. The increased noise floor at $k = 1$ is a known artifact where the folding transformation's Jacobian ($\frac{1}{\tilde{r}^2}$) amplifies numerical noise from the slowly decaying $\frac{1}{\tilde{r}^2}$ tail of the corresponding $P_{\mathrm{P}}^{(1)}(\tilde{r})$ distribution.

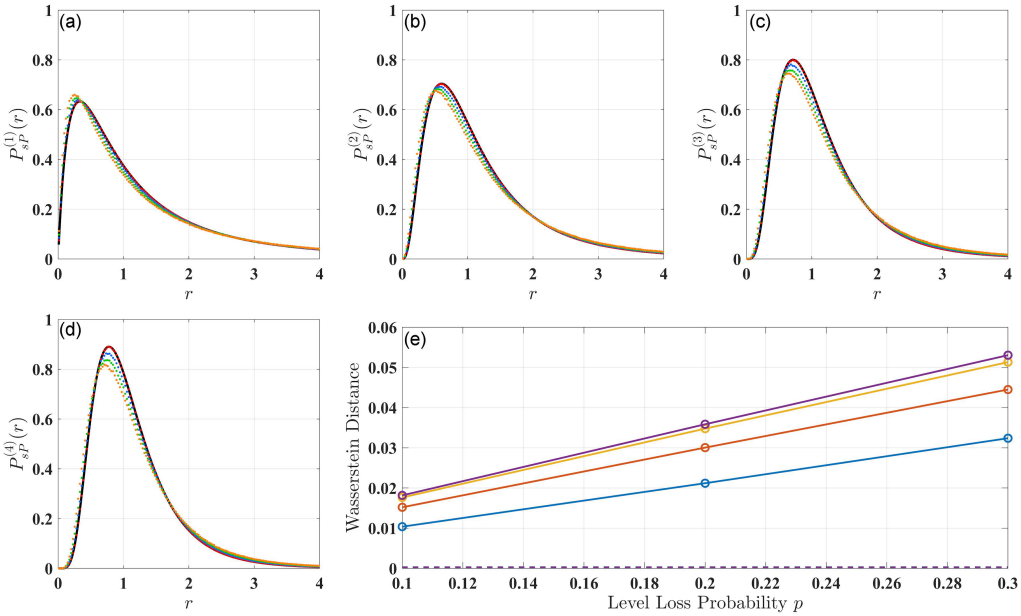

Fig. 3. Sensitivity of the semi-Poisson distribution $P_{\mathrm{sP}}^{(k)}(r)$ to missing levels. Panels (a)–(d) display the distributions $P^{(k)}(\tilde{r})$ for orders $k = 1, 2, 3, 4$. For all k, the numerical distributions for level loss probabilities ($p = 0.1$ (blue dots), $p = 0.2$ (green dots), and $p = 0.3$ (orange dots)) systematically detach from the analytical curve (solid black line) and the corresponding numerical ($p = 0$) curve (red dots). The summary plot (panel (e)) shows the Wasserstein distance as a function of the level loss probability p. The dashed lines indicate the extremely low $W(p = 0)$ noise floor corresponding to k. A clear, monotonic increase is observed in the solid trend lines, thus confirming the instability of semi-Poisson statistics when levels are missing.

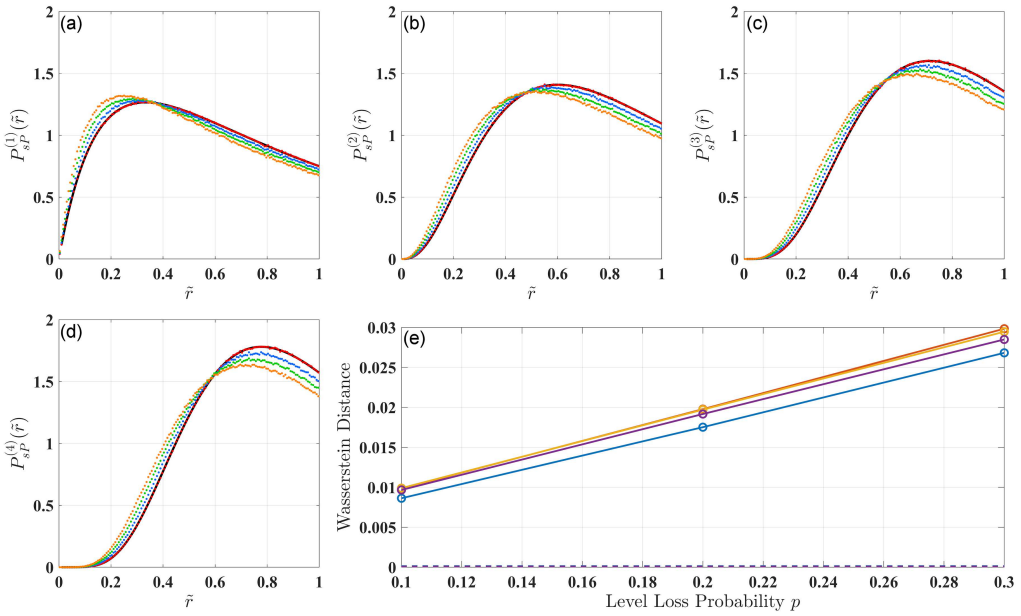

Fig. 4. Sensitivity of the semi-Poisson folded distribution $P^{(k)}(\tilde{r})$ to missing levels. Panels (a)–(d) display the distributions for orders $k = 1, 2, 3, 4$. The distortion of the distributions with increasing level loss probability p is evident, as the curves for $p > 0$ ($p = 0.1$ (blue dots), $p = 0.2$ (green dots), and $p = 0.3$ (orange dots)) consistently departure from the analytical curve (solid black line) and the corresponding numerical ($p = 0$) data (red dots). The summary plot (panel (e)) shows the Wasserstein distance as a function of p. The dashed lines represent the minuscule $W(p = 0)$ noise floor. The solid trend lines (blue, orange, yellow, and purple for $k = 1, 2, 3$, and 4, respectively) demonstrate a strong, monotonic increase, confirming the folded distribution's high sensitivity to missing levels in semi-Poisson ensembles.

TABLE II

Mean Wasserstein distances for the $P(r)$ representation. Values are averaged over $p \in \{0.1, 0.2, 0.3\}$ and 200 realizations.

k	W_{P}	W_{sP}	$W_{\mathrm{sP}}/W_{\mathrm{P}}$
1	0.00045 ± 0.00019	0.02118 ± 0.00023	47
2	0.00060 ± 0.00019	0.02993 ± 0.00022	50
3	0.00039 ± 0.00012	0.03462 ± 0.00023	89
4	0.00038 ± 0.00014	0.03572 ± 0.00025	94

TABLE III

Mean Wasserstein distances for the $P(\tilde{r})$ representation. Values are averaged over $p \in \{0.1, 0.2, 0.3\}$ and 200 realizations.

k	W_{P}	W_{sP}	$W_{\mathrm{sP}}/W_{\mathrm{P}}$
1	0.00515 ± 0.00013	0.01780 ± 0.00013	2.3
2	0.00030 ± 0.00010	0.01981 ± 0.00012	66
3	0.00014 ± 0.00007	0.01968 ± 0.00012	141
4	0.00015 ± 0.00008	0.01910 ± 0.00013	127

This leads to an increased noise floor, making the $k = 1$ folded ratio an inaccurate reference point. Nonetheless, for all higher orders ($k > 1$), where the distributions exhibit fast declining tails, this instability vanishes, and $P_{\mathrm{P}}^{(k)}(\tilde{r})$ becomes an extremely sensitive and robust probe. This finding strongly supports the use of higher-order ratios ($k > 1$).

The response of the Poisson ensemble in the presence of missing levels was investigated using both $P_{\mathrm{P}}^{(k)}(r)$ and $P_{\mathrm{P}}^{(k)}(\tilde{r})$. As shown in Figs. 1 and 2, in the individual panels (a)–(d) for orders $k = 1, 2, 3$, and 4, respectively, the numerical curves for different missing level fractions ($p = 0, 0.1, 0.2$, and 0.3) are statistically indistinguishable, collapsing onto a single curve that aligns well with the analytical prediction. This stability is confirmed by a quantitative analysis employing the Wasserstein distance ($W_{\mathrm{P}}(p)$), which illustrates the distance as a function of the level loss probability. For $P_P^{(k)}(r)$, the measured $W_{\mathrm{P}}(p)$ remains consistently on the order of 10^{-4} for all k (refer to Table II. These values are comparable to the computed noise floor. The trend lines for $p > 0$ show that the Wasserstein distance remains consistently at this extremely low level (see Fig. 1e)). The minor fluctuations are non-monotonic and do not show any systematic increase with p. The analysis of $P_{\mathrm{P}}^{(k)}(\tilde{r})$ provides further substantial evidence supporting $k > 1$ (see Fig. 2). For $k = 2, 3$, and 4, the stability is even more pronounced. As shown in Fig. 2e, the Wasserstein distances are extremely small, matching their noise floor values, and the trend lines are perfectly flat. As presented in Table II, in the case $k = 1$, $W_{\mathrm{P}}(p)$ is on the order of 10^{-3}. This does not indicate physical instability, but rather a known numerical artifact of the folding transformation. Interestingly, despite the increased baseline, the trend line for $k = 1$ remains perfectly flat, demonstrating that this distribution is stable even in the presence of missing levels.

The semi-Poisson ensemble shows a clear response to random level loss, unlike the Poisson ensemble. The results for both $P_{\mathrm{sP}}^{(k)}(r)$ and $P_{\mathrm{sP}}^{(k)}(\tilde{r})$ distributions are presented in Figs. 3 and 4, respectively. The primary observation of the individual k-panels reveals a systematic departure of the distributions from the analytical prediction. For all orders k and both distributions, the numerical curves for spectra with missing levels ($p > 0$) clearly detach from the analytical curve and the corresponding numerical $p = 0$ data. As shown in Fig. 3, the peak of the distribution shifts to the left, and its height is suppressed with increasing probability of level loss p and orders k, indicating a qualitative change in the underlying statistics. This deviation is confirmed by a quantitative analysis using the Wasserstein distance $W_{\mathrm{sP}}(p)$, which is evaluated as a function of the missing level fraction (see Tables II and III). The plots show a steep, monotonic increase of $W_{\mathrm{sP}}(p)$ with p. The panels (e) in Figs. 1 and 2 demonstrate that, starting from a baseline noise floor on the order of 10^{-4}, the distance grows substantially with p. For instance, when 30% ($p = 0.3$) of levels are missing, the distance reaches values on the order of 10^{-2}. The impact of these missing levels is amplified at higher orders k. The trend line's slope in both distributions exhibits an increase as k rises.

5. Conclusions

In this work, we have investigated the impact of randomly missing levels on the higher-order spacing ratio statistics for both Poisson and semi-Poisson ensembles. Our goal was to address a fundamental challenge in the analysis of quantum spectra — the ambiguity that arises when attempting to classify a system with missing levels. By analyzing the stability of the $P^{(k)}(r)$ and $P^{(k)}(\tilde{r})$ distributions under a controlled removal of levels, we have uncovered a clear and robust diagnostic signature. We have shown that the entire family of higher-order distributions for the Poisson ensemble is stable against missing levels. The Wasserstein distance between the distribution of a spectrum with missing levels and the ideal analytical distribution remains at the simulation's noise floor (10^{-4}) and is independent of the fraction of missing levels. However, the semi-Poisson ensemble demonstrates considerable statistical instability. As missing levels rise, the Wasserstein distance increases monotonically, quickly surpassing the baseline noise floor and reaching values on the order

of 10^{-2}. This demonstrates that the short-range correlations characterizing the semi-Poisson ensemble are sensitive to information loss. Additionally, we have demonstrated that the instability is amplified at higher orders k, suggesting that the effective longer-range correlations are even more sensitive to disruption. Also, we found $P^{(k)}(\tilde{r})$ to be a more reliable and sensitive probe, providing a higher signal-to-noise ratio for observing these effects, particularly when $k > 1$. For instance, in $P^{(3)}(\tilde{r})$ distribution, the statistical change induced by level loss in the semi-Poisson ensemble (W_{sP}) is over 140 times greater than the baseline numerical noise observed in the stable Poisson case (W_{P}). The primary implication of our work is that the stability of spectral statistics under artificial removal of levels serves as a robust, model-independent diagnostic tool. We can firmly conclude the presence or absence of underlying correlations by examining how higher-order distributions of a measured spectrum behave when removing levels.

Acknowledgments

A.A. acknowledges support from the National Science Centre, Poland, Grant No. 2024/53/B/ST2/00144.

References

[1] F. Haake, *Quantum Signatures of Chaos*, 3rd. ed., Springer-Verlag, New York 2010.

[2] O. Hul, S. Bauch, P. Pakoński, N. Savytskyy, K. Życzkowski, L. Sirko, *Phys. Rev. E* **69**, 056205 (2004).

[3] L. Sirko, P.M. Koch, R. Blümel, *Phys. Rev. Lett.* **78**, 2940 (1997).

[4] Y. Hlushchuk, A. Błędowski, N. Savytskyy, L. Sirko, *Phys. Scr.* **64**, 192 (2001).

[5] O. Bohigas, M.J. Giannoni, C. Schmit, *Phys. Rev. Lett.* **52**, 1 (1984).

[6] M.L. Mehta, *Random Matrices*, Academic Press, New York 1991.

[7] M. Ławniczak, S. Bauch, O. Hul, L. Sirko, *Phys. Scr.* **T135**, 014050 (2009).

[8] O. Hul, P. Šeba, L. Sirko, *Phys. Rev. E* **79**, 066204 (2009).

[9] M. Ławniczak, S. Bauch, O. Hul, L. Sirko, *Phys. Scr.* **T147**, 014018 (2012).

[10] M. Ławniczak, S. Bauch, O. Hul, L. Sirko, *Phys. Scr.* **T143**, 014014 (2011).

[11] O. Farooq, A. Akhshani, M. Ławniczak, M. Białous, L. Sirko, *Phys. Rev. E* **110**, 014206 (2023).

[12] A. Rehemanjiang, M. Allgaier, C.H. Joyner, S. Müller, M. Sieber, U. Kuhl, H.-J. Stöckmann, *Phys. Rev. Lett.* **117**, 064101 (2016).

[13] J. Lu, J. Che, X. Zhang, B. Dietz, *Phys. Rev. E* **102**, 022309 (2020).

[14] M. Ławniczak, A. Akhshani, O. Farooq, M. Białous, S. Bauch, B. Dietz, L. Sirko, *Phys. Rev. E* **107**, 024203 (2023).

[15] M. Ławniczak, A. Akhshani, O. Farooq, S. Bauch, L. Sirko, *Acta Phys. Pol. A* **144**, 469 (2023).

[16] M.V. Berry, M. Tabor, *Proc. R. Soc. London Ser. A* **356**, 375 (1977).

[17] E.B. Bogomolny, U. Gerland, C. Schmit, *Phys. Rev. E* **59**, R1315 (1999).

[18] E. Bogomolny, O. Giraud, C. Schmit, *Phys. Rev. E* **65**, 056214 (2002).

[19] A. Akhshani, M. Białous, L. Sirko, *Phys. Rev. E* **108**, 034219 (2023).

[20] E. Bogomolny, C. Schmit, *Phys. Rev. Lett.* **93**, 254102 (2004).

[21] A.L. Corps, R.A. Molina, A. Relaño, *SciPost Phys.* **10**, 107 (2021).

[22] R.A. Molina, J. Retamosa, L. Muñoz, A. Relaño, E. Faleiro, *Phys. Lett. B* **644**, 25 (2007).

[23] O. Morales, Irving, E. Landa, P. Stránský, A. Frank, *Phys. Rev. E* **84**, 016203 (2011).

[24] V. Oganesyan, D.A. Huse, *Phys. Rev. B* **75**, 155111 (2007).

[25] Y.Y. Atas, E. Bogomolny, O. Giraud, G. Roux, *Phys. Rev. Lett.* **110**, 084101 (2013).

[26] Y.Y. Atas, E. Bogomolny, O. Giraud, P. Vivo, E. Vivo, *J. Phys. A Math. Theor.* **46**, 355204 (2013).

[27] A. Akhshani, M. Białous, L. Sirko, *Phys. Rev. E* **112**, 014201 (2025).

[28] S.H. Tekur, M.S. Santhanam, *Phys. Rev. Res.* **2**, 032063(R) (2020).

[29] M. Ławniczak, M. Białous, V. Yunko, S. Bauch, B. Dietz, L. Sirko, *Acta Phys. Pol. A* **132**, 1672 (2017).

[30] M. Białous, B. Dietz, L. Sirko, *Acta Phys. Pol. A* **140**, 545 (2021).

[31] M. Białous, B. Dietz, L. Sirko, *Phys. Rev. E* **103**, 052204 (2021).

[32] A. Ramdas, N.G. Trillos, M. Cuturi, *Entropy* **19** (2017).

[33] C.-C. Pan, X. Dong, Y.-C. Sun, A.-Y. Cheng, A.-B. Wang, Y.-X. Hu, H. Cai, W. Wang, *Phys. Rev. D* **111**, 096017 (2025).

[34] U.T. Bhosale, *Phys. Rev. B* **104**, 054204 (2021).

[35] W.-J. Rao, M.N. Chen, *Eur. Phys. J. Plus* **136**, 81 (2021).

[36] O. Bohigas, M.P. Pato, *Phys. Rev. E* **74**, 036212 (2006).

[37] M. Ławniczak, M. Białous, V. Yunko, S. Bauch, L. Sirko, *Phys. Rev. E* **98**, 012206 (2018).